DOI:
10.1016/j.jddst.2019.03.032

Document Version
Peer reviewed version

Enhanced antitubercular activity, alveolar deposition and macrophages uptake of mannosylated stable nanoliposomes

Amira Hamed[1], Rihab Osman[1], Khuloud T. Al-Jamal[2], Samar Mansour Holayel[1,3], Ahmed-Shawky Geneidi[1]

[1]Department of Pharmaceutics and Industrial Pharmacy, Faculty of Pharmacy, Ain Shams University, Abbassia, Cairo, Egypt; [2]Institute of Pharmaceutical Science, Faculty of Life Sciences & Medicine, King's College London, Franklin-Wilkins Building, 150 Stamford Street, London SE1 9NH, United Kingdom.[3]Department of Pharmaceutical Technology, Faculty of Pharmacy and Biotechnology, German University in Cairo, Cairo, Egypt.

Abstract

Two targets were set for the current work: exploiting the effect of the targeting ligand 4-aminophenyl-alpha-D–manno-pyranoside (PAM) in enhancing the uptake of nanoliposomes (NL) by alveolar macrophages and investigating the efficiency of NL *co*-spray drying with the carrier biomacromolecule dextran (DX) for improved physical stability and lung deposition. Moxifloxacin (MXF) loaded NL were prepared by reversed phase evaporation method using different lipids and the surface of selected NL was decorated with PAM. Selected NL formulations were *co*-spray dried with dextran (DX) to yield surface modified NL embedded in microparticles (SD-NLEM). Using the proportion method, the antibacterial activity against resistant *M. tuberculosis* was tested. The safety of the developed system was tested on lung cancer cells and the uptake by alveolar macrophages was followed using flow cytometry measurements. Fluorescently labeled NL were tracked *in vivo* in rats to test lung deposition following pulmonary administration. The results showed that spray drying efficiently enhanced the stability and morphological characteristics of the optimized monodisperse NL achieving a respirable particle fraction of more than 75%. Deep lung deposition was confirmed in rats. Charged NL provided higher anti-tubercular activity and macrophage uptake compared to the neutral ones. Mannosylation efficiently increased active uptake by alveolar macrophages uptake.

Keywords: Nanoliposomes; lung targeting; macrophages; spray drying; aminophenyl-manno-pyranoside; microparticles; tuberculosis.

List of abbreviations

AE	Association efficiency
CFU	Colony forming unit
CH	cholesterol
d	Geometric mean diameter
DCP	Dicetyl phosphate
DMSO	Dimethyl sulphoxide
DOTAP	N-[1-(2, 3- dioleoyloxy)propyl]-N,N,N-trimethyl ammonium chloride
DX	Dextran sulphate
EE	Encapsulation efficiency
EF	Emitted fraction
EI	Effective inhalation index
FBS	Fetal bovine serum
FI	Fkuorescence intensity
FITC	Fluorescein isothiocyanate
FPF	Fine particle fraction
Leu	Leucine
m_{empty}	Mass of the capsule after simulating the inhalation
m_{full}	Mass of the capsule before simulating the inhalation
MIC	Minimal inhibitory concentration
MMAD	Mass median aerodynamic diameter
MP	Microparticles
m_{powder}	Mass of the powder in the capsule
MXF	Moxifloxacin hydrochloride
NL/C	NL to carrier ratio
NLEM	Nanoliposomes embedded in microparticles
PAM	4-aminophenyl-alpha-D–manno-pyranoside
PBS	Phosphate buffer solution
PC	L-α-phosphatidylcholine
PE	Phosphatidyl-ethanolamine
PS	Particle size
rpm	Revolutions per minute
SD	Spray dried
SEM	Scanning electron microscopy
St2	Fraction (%) distributed to stage 2
TEM	Transmission electron microscope
TSI	Twin stage glass impinger
VMD	Volume mean diameter
$W_{free\ drug}$	Amount of free drug detected in supernatant
$W_{initial\ drug}$	Total amount of the drug used
ζ	Zeta potential
λ_{max}	Wavelength of maximum absorption
ρ	Tapped density
ρ_0	Reference density of $1 g/cm^3$

1. Introduction

Tuberculosis (TB), the second most common cause of death worldwide is caused by the gram positive aerobic intracellular bacteria, mycobacterium tuberculosis *(M. tuberculosis)* **[1]**. Although, it affects many organs yet, in 80% of cases, the disease is confined to the lung causing a severe lifelong communicable respiratory infection called pulmonary TB. The efficacy of therapy of TB is usually constrained by drug dosage, first pass effect, systemic adverse effects specifically reduced liver and kidney functions, inadequate distribution to pathological sites, in addition to the emergence of drug resistance. The residence and proliferation of *M. tuberculosis* in alveolar macrophages (AM), within secreted waxy complex cellular envelope, resisting treatment, contribute to the difficulty of tuberculosis eradication **[2, 3]**.

Inhalation therapy has emerged as a valuable approach for the site specific treatment **[2-5].** However, for effective lung targeting, specific attributes of size, surface characteristics, and aerodynamic properties with the ability to evade the lung defense mechanisms should be considered while designing the carrier [6]. In this context, liposomes exhibit potential characteristics for lung delivery. Beside their biocompatibility, amphiphilic character, biodegradability, and low immunogenic potential, liposomes are formulated from natural or synthetic phospholipids that are similar to endogenous lung surfactant which make them an ideal pulmonary delivery carrier **[7]**. With the versatility of phospholipid molecules used for their fabrication, it has been possible to tailor liposomes with specific particle size (PS), surface charge and physiochemical characteristics to passively target a particular region in the RT, in this study the alveolar macrophages (AM) **[8]**.

Moxifloxacin hydrochloride (MXF) is a fourth generation fluoroquinolone with dual antimicrobial mechanism of action **[9]**. It is effective against drug susceptible and multi drug resistance TB **[10, 11]** . Encapsulation of MXF in vesicular delivery systems was thought to improve the efficiency of TB treatment. Anchoring a mannose derivative on the NL surface is thought to boost the macrophage targeting efficiency besides the specially designed liposomes characteristics.

However, poor scale-up, cost, short shelf life, and in some cases toxicity are among reported liposomes shortcomings **[12]**. To enhance their stability and meet the aerodynamic characteristics, inherently required for lung targeted delivery systems, spray drying of liposomes using suitable carriers that can preserve them during dehydration, offers an attractive option to provide dry microparticles (MP) suitable for inhalation **[8, 13]**. Upon contact with pulmonary fluid these MP dissociate into NL, combining the ability of MP lung deposition with NL advantages **[14].**

Hence, the ultimate target of this work was to ensure the fabrication of stable liposomes encapsulating MXF with efficient lung delivery characteristics. We hypothesized that by tuning the size, charge, composition of liposomes as well as anchoring surface ligand, PAM, better targeting of antitubercular drugs to the AM could be achieved. *Co*-spray drying NL with a biocompatible fast dissolving polysaccharide, dextran, was implied to enhance physical stability and lung delivery characteristics **[6].** Comparative studies relating *in vitro* lung deposition using a twin stage impinger to *in vivo* deposition using a dry powder insufflator is also presented in this work. The developed targeted nanocarrier platform is expected to have great potential for improving drug cure in case of intracellular infectious diseases.

2. Materials and methods

2.1. Materials

Moxifloxacin hydrochloride (MXF) was kindly provided by Medical Union Pharmaceuticals Company (Egypt). L-α-phosphatidylcholine (PC), type X-E, from dried egg yolk, cholesterol (CH), dicetyl phosphate (DCP), 4-aminophenyl-alpha-D–manno-pyranoside (PAM), glacial acetic acid and phosphotungstic acid were from Sigma (UK). N-[1-(2, 3-dioleoyloxy)propyl]-N,N,N-trimethyl ammonium chloride (DOTAP) and phosphatidyl-ethanolamine (PE) from egg yolk were from Lipoid (Germany). Dextran sulphate (DX) (MW 500,000), dimethyl sulphoxide (DMSO) ≥99.9% and fluorescein isothiocyanate (FITC) from Sigma (UK). Leucine from Fluka, (Switzerland). Glutaraldehyde solution, 25% in water, from Chemie GmbH, Germany. All other chemicals and reagents were of analytical grade.

2.2. Preparation of MXF- loaded nanoliposomes (MXF-NL)

Various phospholipids, PC or PC/PE, to CH molar ratios were used for the preparation of liposomes applying the modified reverse phase evaporation (REV) method **[15].** DCP and DOTAP were used to impart negative and positive charge, respectively **[16-18]**. Briefly, lipids were dissolved in 2:1v/v chloroform/methanol mixture in a round bottom flask at a concentration of 2%w/v and the organic solvent was removed by rotary evaporator (Janke and Kunkel, IKA Laboratories, Staufen, Germany) at 40˚C. The obtained film was dissolved in 12 mL diethyl ether and MXF, dissolved in 10 mL PBS, pH 7.4, was added to the lipid mixture which was bath-sonicated for 5 min. The organic solvent was again removed under reduced pressure at 40˚C using a rotary evaporator, rotating at approximately 200 rpm, until a gel was formed. Upon further vigorous rotary evaporation (300 rpm), the resultant gel was broken to give the liposomes. The remaining aqueous phase (16 mL PBS, pH 7.4) was then added portion wise with gentle vortex mixing. Then the flask was stirred at ambient temperature on rotary evaporator at 200 rpm for 45 min. The formed liposomes were passed through a stack of polycarbonate membrane with defined pore size (400nm) using an extruder (Lipex extruder, Avestin Inc.). The liposome suspension was left to mature overnight at 4˚C to ensure hydration of the lipid. The effect of varying the buffer pH was also evaluated. **Table 1** shows the composition of the developed formulae.

2.3. Preparation of MXF loaded mannosylated NL (MXF-PAM-NL)

The targeting biomacromolecule PAM was conjugated to the optimum PE containing NL adopting gluteraldehyde cross-linking method **[19, 20]**. Briefly, an amount of 1mL of liposomal dispersion in PBS, pH 7.4, was mixed with 2mL of 1% w/v aqueous PBS solution of PAM. Glutaraldehyde was added slowly to the liposomal suspension at a final concentration of 3mM and the mixture was incubated for 5min at 20˚C **[20]**. Dynamic dialysis technique against 1liter PBS solution at room temperature was performed to remove the uncoupled glutaraldehyde with replacement of PBS every 30min **[21]**.

2.4. Preparation of spray dried nanoliposomes embedded in microparticles (SD-NLEM)

Freshly prepared NL were dispersed in 50mL deionized water containing 10mg/mL of the biomacromolecular carrier (DX) as bulking agent ± Leu as dispersing aid. The dispersions were then spray dried using a Buchi-290 spray dryer (Buchi Laboratorium, AG, Switzerland) at air flow

rate of 473 L/h and a nozzle atomizer diameter of 0.7mm. A pump capacity of 5% and aspiration rate of 85% at an inlet temperature of 80˚C were applied. The spray dried powders (SDP) were collected and stored in a vacuum desiccator at room temperature for further analysis.

2.5. NL characterization

2.5.1. Determination of drug encapsulation efficiency (EE)

Drug EE in NL was determined indirectly by measuring the concentration of the free drug in the supernatant following centrifugation of NL dispersion placed in *Nanosep®* (MWCO 100KDa; Pall Life Sciences, USA), at 9000rpm for 90min at 4˚C in a cooling centrifuge (Bench Biofuge, Heraeus, Germany). The amount of free MXF in the supernatant was estimated spectrophotometrically at predetermined $\lambda_{max,}$ (289nm), using UV-visible spectrophotometer (Model UV-1601PC; Shimadzu, Kyoto, Japan.) and EE was calculated according to the following equation:

$$EE\% = \{(W_{initial\ drug} - W_{free\ drug})/ W_{initial\ drug}\} \times 100 \qquad (1)$$

Where "$W_{initial\ drug}$" is the total amount of the drug used and "$W_{free\ drug}$" is the amount of free drug detected in supernatant after centrifugation of the aqueous dispersion.

2.5.2. Particle size (PS) and zeta potential (ζ) determination

PS analysis and ζ were determined using Zetasizer Nano ZS (Malvern Instruments Ltd, Malvern, UK) as previously described elsewhere.

2.5.3. Morphological examination by transmission electron microscope

A drop of NL dispersion was applied on carbon-coated copper grid for 2–3min and the excess was then drawn off with filter paper **[22]**. A drop of 2% (w/v) phosphotungstic acid was subsequently placed to the grid. Negatively stained NL were examined by TEM (Hitachi-H-600, electron microscope, Jeol, Japan), at a power of 120 kV.

2.5.4. Proton magnetic resonance (^{1}H-NMR)

The incorporation of PAM in the NL was confirmed by ^{1}H-NMR. The prepared NL, purified by dialysis, were then separated by centrifugation using *Nanosep*®, left to air dry and then dissolved in DMSO by vortex mixing for 48h. The ^{1}H-NMR scan was done at a frequency 400MHz, pulse width 12W and scan number 16.

2.6. SD-NLEM characterization

The spray drying yield and powder moisture content were determined according to methods described in supplementary information (SI) section **[23].**

2.6.1. PS determination and mass median aerodynamic diameter calculation

PS was determined adopting the wet dispersion method using Laser diffraction-Malvern Mastersizer S (Malvern instrument-UK). Isopropanol was employed isopropanol as antisolvent and PS was expressed as the volume mean diameter (VMD) and the span **[7, 24]**. The mass median aerodynamic diameter (MMAD) was then calculated according to the following equation.

$$\text{MMAD} = d\sqrt{\rho/\rho 0} \qquad (2)$$

Where d is the geometric mean diameter obtained from PS analysis, ρ is the tapped density and ρ_0 is the reference density of 1g/cm^3 **[25]**. Selected MXF loaded SD-NLEM were stored in desiccator over silica gel at room temperature for six months. Samples from each batch were withdrawn at specified time intervals to determine the PS.

2.6.2. NL recovery from SD-NLEM

An amount of 10mg of SDP was dispersed in 3mL of PBS, pH 7.4 and vortexed for 1min. The size of the dispersed particles S_f was determined using Zetasizer and was compared to the initial size of the NL before spray drying (S_i). The value of S_f/S_i ratio close to unity indicates full redispersibility **[26-28].**

2.6.3. Drug association (AE) and encapsulation efficiency (EE) determination

An accurately weighed amount of SDP was dissolved in 30%v/v aqueous methanolic solution and the AE was determined as % from theoretical drug content. EE of MXF in SD-NLEM

was determined indirectly by measuring the concentration of the free drug in the aqueous phase following re-dispersion of an accurately weighed amount of SDP in PBS, pH 7.4.

2.6.4. In vitro aerodynamic deposition of SD-NLEM

The aerodynamic deposition was evaluated using the twin stage glass impinger (TSI) (Copley, Nottingham, UK). The upper and lower impingement chambers of the TSI were filled with 7 and 30mL of 30% v/v methanol in water, respectively. Aliquot of the SDP (15mg) was loaded in HPMC No 3 capsules and placed in the *Aerolizer*®, attached to the throat of the impinger *via* the adaptor and the test was performed as previously described **[5, 29]**. Drug content of the powder collected on each stage was determined spectrophotometrically. *In vitro* aerosolization properties of the SDP was described by the following terms: emitted fraction EF, determined gravimetrically, and defined as the total amount of powder emitted from the inhaler as a percentage of the amount of powder loaded in the capsule, expressed as:

$$EF = \frac{(m\ full - m\ empty)}{m\ powder} x100 \qquad (3)$$

Where m_{full} and m_{empty} are the masses of the capsule before and after simulating the inhalation respectively and m_{powder} is the mass of the powder. Respirable particle fraction (RP), which is a percentage of drug deposited on lower stage of TSI against the particles emitted from the inhalation system (emitted fraction) and effective inhalation index (EI), were also calculated using the following equations:

$$RP\ \% = (St2/Em)x100 \qquad (4)$$

$$EI\ \% = \sqrt{St2xEm} \qquad (5)$$

Where Em is the fraction (%) emitted from the inhalation system, and St2 is the fraction (%) distributed to stage 2 of the TSI. For an ideal DPI, the EI and RP are 100% ***[30]***.

2.6.5. Surface morphology of SD-NLEM

The surface morphology of selected SDP was examined using scanning electron microscopy; SEM (Model Quanta 250 FEG, FEI company, Netherlands) as previously described **[7].**

2.6.6. In vitro MXF release from SD-NLEM

In vitro MXF release was performed adopting the dialysis membrane diffusion technique. Briefly, an accurately weighed amount of SD-NLEM was suspended in 0.5mL PBS (pH=7.4) in a dialysis bag immersed in vial containing 3mL PBS (pH 7.4). The vials were placed in a shaking water bath at 37±0.5°C rotating 50strokes/min. At predetermined time intervals, samples were withdrawn, replaced with fresh buffer, and assayed spectrophotometrically at 295 nm for MXF content.

2.6.7. Antibacterial activity of MXF-NLEM

The antibacterial effectiveness of blank and MXF-NLEM was assessed in comparison to the free drug by measuring the minimal inhibitory concentration (MIC) against *M. tuberculosis*. The proportion method using Lowenstein-Jensen medium was adopted **[31].** The MIC (µg/mL), the lowest concentration that inhibited more than 99% of visible bacterial growth of initial inoculum, was determined by counting the number of colony forming unit (CFU) in each vial and comparing them with the growth in the control vial **[32]**. The experiment was performed in triplicate.

2.6.8. Cytotoxicity evaluation by MTT assay

Cytotoxicity of selected formulae was evaluated using MTT assay on lung cancer cells (A549) **[33]**. Serial two fold dilutions from 25 to 0.78µg/mL of the drug solution, equivalent amounts of drug loaded formulae and their blanks were prepared. A control of untreated cells was made in the absence of test compound. The absorbance of untreated cells was considered as 100%. The results were determined by three independent experiments performed in triplicate (n=9) and the cell viability was calculated as previously described **[34, 35].**

2.6.9. In vitro phagocytosis of NL using mice macrophages J774A.1

FITC-labeled NL were first prepared as previously described while replacing MXF solution by FITC solution (0.2mg/mL). Dynamic dialysis technique against PBS solution at room temperature, until no fluorescence was detected in the dialysate, was performed to remove the unentrapped FITC.

Murine monocytes macrophages of cell line J774A.1 were used to study the potential of macrophage uptake of NLEM. The cells were maintained in complete medium consisting of DMEM supplemented with10% fetal bovine serum (FBS), 2mM-glutamine and 0.1%w/v penicillin-streptomycin solution and incubated at 37˚C and 5% CO_2 atmosphere. Aliquots (500µL) of J774A.1 cells ($5x10^4$) cells were seeded in each well of a 24 wells plate on glass cover slips coated with poly-D-lysine. The plate was incubated for 24h and then washed with DMEM-L-glutamine to remove non-adherent cells. Subsequently 500µL of DMEM-L-glutamine containing 0.25 or 0.5mg/mL of FITC- SD-NLEM (corresponding to lipid concentrations 75 and 150µg/mL) were added to the cells in each separate well. The cells were incubated with the particles for 30 or 180 min **[36]**. The medium was then aspirated and the cells were washed twice with PBS to remove the particles adhering to the cell surface. Subsequently the cells were fixed with 4% paraformaldehyde solution for 30min at room temperature then washed twice with PBS. The cells associated fluorescence was measured by fluorescence activated cell sorter (FACS) (BD Biosciences). Cells incubated without addition of FITC loaded particles were used as control to determine the auto-fluorescence. Fluorescence intensity was used as indicator of the amount of cellular uptake.

2.6.10. In vivo pulmonary deposition study

For all animal studies, the experimental procedures conformed to the Ethics Committee of Faculty of Pharmacy, Ain Shams University on the use of animals. Male albino rats were housed in an environment with a controlled temperature (21-24˚C) and lighting (12:12h light-darkness cycle).

In vivo deposition studies of FITC-loaded SD-NLEM were performed as previously reported **[37, 38].** An accurately weighed dose of about 5mg of FITC-loaded SD-NLEM (formula SD-PC) were delivered intra-pulmonary using the low scale dry powder inhaler (DPI) (Model DP-

4 from *Penn-century®)*. The rat's abdominal cavity was incised immediately after powder administration, then a catheter connected to an infusion pump was inserted in the posterior vena cava. The lungs were treated consecutively with two infusion solutions. The first infusion was done at a rate of 10mL/min for 5min with PBS pH7, then the lung was perfused with 4% formaldehyde at 5mL/min for 5min for fixation. The lung was then removed and cross sectioned (section thickness~30µm). For each part (trachea, bronchus, bronchioles and alveolar ducts), 3-5 slides were prepared and examined by fluorescent microscope (Olympus U-RFL-T, BX51, Olympus, Berlin, Germany) **[38]**. A control experiment was run to assess the auto-fluorescence of rat lung tissue in which rat had not received any powder and tissues were rinsed and fixed as mentioned above.

2.7. Statistical analysis

All formulations were prepared and reported in triplicate. Results are expressed as mean ± s.d. (standard deviation).The statistical significances of difference between groups were evaluated by one-way ANOVA and Tukey's post hoc test with a significance level of $p<0.05$.

3. Results and discussion

3.1 Optimized MXF–NL using various lipids

Trying various PC/CH molar ratios (10:0, 9:1, 8:2, 7:3, 6:4, and 5:5) for the preparation of MXF-NL revealed that the absence of CH in the formulation led to high PS (371.98 ±6.98nm) and PDI (0.645 ±0.039) with low EE (27.45±3.57%), **Table 1**. Smaller PS and PDI were seen following its incorporation, **Fig.1S**. CH increases stability and rigidity of the liposomal membrane during hydration, enhances microviscosity of the lipid bilayer, reduces permeability and acts as crystal-breaker of the gel phase and induces of chain-ordering in the fluid phase without rigidification of the overall phase **[39, 40]**. Increasing CH level, up to PC/CH molar ratio7:3, led to significant EE increase ascribed to the ability of CH to cement the leaking spaces in the phospholipid bilayers. Conversely, at higher CH level (PC/CH 6:4 and 5:5), the EE decreased probably due to a disruption in the regular bilayer structure leading to leaching of drug lowering

its entrapment **[41-43]**. Hence, a molar ratio of (7:3) of PC/CH was found optimum; at this level, the highest EE (66.25±1.89%) was seen with a MXF to total lipids ratio of 0.15:1.

The use of PE caused significant PS increase as evidenced by comparing PE1 to PC8. Increase PE conc resulted in slight significant increases in PS and EE as seen in PE2, followed by formation of a heterogenous liposomal dispersion with higher PDI (0.483±0.049) and PS (580.5±11.53nm) and lower EE (53.32 ±1.89%), as seen with PE3. The reported instability of PE and its rapid phase transition to non-bilayer (hexagonal phase II) structures could account for this observation **[20]**. This was probably overcome by the stabilising effect of PC and CH at lower PE/PC ratios **[39]**. The noted decreased ζ in PE formulae especially PE3 might also have contributed to the liposomes instability and aggregation. Formula PE2 was selected for subsequent surface modification with PAM.

Various PC/DCP ratios were used to prepare anionic at 7:3 lipid /CH ratio. No significant difference *($p>0.05$)* was seen in PS while a significant *($p<0.05$)* reduction in EE was noted. Decreasing the pH to 5.5 led to a slight, though significant, increase in EE which reached 62.05 ±2.19%. The ionization of MXF amino group at pH 5.5 resulted probably in a strong electrostatic attraction between the negatively charged DCP and the drug cation **[44]**, an effect which was not seen with other lipids. A higher negative ζ compared to formula PC prepared without DCP pointing out to their possible higher stability.

DOTAP alone or in combination with PC was used to prepare cationic MXF-NL. The lowest PDI (0.242 ±0.002) and the highest MXF EE (56.62±2.44%), were seen with DP3 prepared with DOTAP/PC/CH ratio of 3.5:3.5:3 at pH 7.4.

Table 1: Composition and characterization of MXF-nanoliposomes.

Variable	pH	Formula	Formula composition		PS (nm)	PDI	EE (%w/w)	ζ (mV)
			PC: PE:DCP:DOTAP: CH (molar ratio)	MFX[(a)]				
PC:CH	7.4	PC1	10:0:0:0:0	0.1	372 (7.0)	0.65 (0.04)	27.45 (3.57)	-7.85 (0.78)
		PC2	9:0:0:0:1	0.1	244 (1.8)	0.56 (0.09)	34.39 (2.19)	-9.84 (0.55)
		PC3	8:0:0:0:2	0.1	265 (2.6)	0.43 (0.01)	50.19 (2.04)	-12.45 (0.74)
		PC4	7:0:0:0:3	0.1	272 (1.6)	0.29 (0.01)	53.94 (2.53)	-12.08 (0.97)
		PC5	6:0:0:0:4	0.1	323 (10.0)	0.39 (0.02)	40.36 (2.02)	-11.12 (0.45)
		PC6	5:0:0:0:5	0.1	380 (12.3)	0.63 (0.05)	35.28 (2.85)	-10.21 (0.81)
MXF loading	7.4	PC7	7:0:0:0:3	0.05	266 (5.8)	0.38 (0.04)	42.07(5.32)	-11.93 (0.55)
		PC8	**7:0:0:0:3**	**0.15**	**277 (2.2)**	**0.30 (0.02)**	**66.25 (1.89)**	**-12.31 (0.76)**
		PC9	7:0:0:0:3	0.2	281 (1.3)	0.29 (0.01)	50.96 (1.57)	-11.52 (0.66)
		PC10	7:0:0:0:3	0.3	285 (2.6)	0.32 (0.03)	33.53 (2.33)	-11.42 (0.51)
PE conc	7.4	PE1	6:1:0:0:3	0.15	299 (4.1)	0.25 (0.01)	61.66 (2.73)	-8.03 (0.35)
		PE2	5:2:0:0:3	0.15	313 (6.0)	0.30 (0.04)	63.59 (2.52)	-6.54 (0.41)
		PE3	4:3:0:0:3	0.15	580 (11.5)	0.48 (0.05)	53.32 (1.89)	-4.25 (0.38)
PC:DCP	7.4	DC1	6:0:1:0:3	0.15	273 (1.2)	0.25 (0.01)	57.58 (2.02)	-31.32 (0.35)
		DC2	5:0:2:0:3	0.15	274 (0.7)	0.26 (0.03)	46.99 (1.62)	-29.51 (1.63)
	5.5	**DC3**	**6:0:3:0:1**	**0.15**	**273 (3.3)**	**0.24 (0.01)**	**62.05 (2.19)**	**-27.82 (2.76)**
PC:DOTAP	7.4	DP1	0:0:0:1:1	0.15	333 (3.3)	0.33 (0.03)	44.47 (1.49)	25.42 (0.28)
		DP2	0:0:0:7:3	0.15	325 (3.8)	0.27 (0.02)	50.61 (1.58)	26.03 (1.76)
		DP3	**3.5:0:0:3.5:3**	**0.15**	**320 (6.4)**	**0.24 (0.01)**	**56.62 (2.44)**	**23.82 (0.64)**
PAM	7.4	**PE-PAM**	**5:2:0:0::3**	**0.15**	**379 (3.6)**	**0.30 (0.05)**	**62.18 (2.08)**	**-4.12 (0.32)**

[(a):] Calculated as mole/mole of total lipids. PC: egg phosphatidylcholine, CH: Cholesterol, PE: phosphatidyl ethanolamine, DCP: dicetyl phosphate, DOTAP: N-[1-(2, 3- Dioleoyloxy) propyl] -N, N, N- trimethyl ammonium chloride, and MXF: moxifloxacin hydrochloride. Results are mean of three determinations (s.d.).formulae selected for subsequent studies are shown in bold.

Table 2: Characteristics of MXF loaded spray dried nanoliposomes embedded in microparticles (MXF-SD-NLEM).

.

Formula	Leu[a] (%w/w)	NL:C[b]	Yield (%w/w)	%EE (f)[c] (%w/w)	AE (%w/w)	D[4, 3] (µm)	Span	MMAD (µm)	Moisture (%w/w)	S_f/S_i	Size increase (%)
S1	0	1:20	46.78 (4.39)	64.75 (1.59)	-	7.32 (0.05)	2.62 (0.29)	4.76 (0.12)		-	-
S2	20		67.25 (4.01)	63.76 (2.01)	-	2.69 (0.03)	0.95 (0.04)	1.62 (0.01)	-	-	-
S3	30		69.37 (5.15)	62.54 (2.47)	-	2.86 (0.04)	1.48 (0.51)	1.47 (0.05)	-	-	-
S4	40		75.19 (2.94)	61.35 (1.87)	-	3.31 (0.02)	1.35 (0.03)	1.78 (0.09)	-	-	-
S5	50		80.21 (3.93)	60.29 (1.94)	-	3.84 (0.19)	1.26 (0.05)	2.04 (0.09)	-	-	-
S6	60		82.29 (5.24)	55.16 (1.32)	-	6.97 (0.09)	1.22 (0.04)	3.73 (0.15)	-	-	-
S7		1:10	78.32 (2.56)	60.56 (2.12)	-	4.23 (0.23)	1.17 (0.05)	2.51 (0.04)	-	1.08 (0.02)	8.21 (1.66)
S8 (SD-PC)		1:7.5	79.13 (1.78)	59.74 (2.01)	92.12 (2.33)	4.66 (0.17)	1.29 (0.03)	2.74 (0.11)	3.06	1.14 (0.02)	14.45 (2.07)
S9		1:5	77.88 (2.91)	56.81 (1.86)	-	5.56 (0.14)	1.35 (0.03)	3.32 (0.09)	-	1.33 (0.01)	33.07 (1.31)
S10	50	1:2.5	79.22 (4.11)	51.01 (3.26)	-	7.16 (0.45)	1.38 (0.03)	4.42 (0.22)	-	1.64 (0.03)	63.79 (3.29)
SD-PE-PAM		1.7.5	74.88 (2.43)	57.62 (2.25)	93.33 (1.29)	6.78 (0.31)	1.26 (0.11)	4.31 (0.13)	3.12	1.14 (0.01)	13.75 (0.27)
SD-DC			79.54 (3.11)	58.22 (2.03)	93.61 (3.26)	5.28 (0.14)	1.27 (0.07)	3.12 (0.11)	3.09	1.13 (0.02)	12.62 (2.08)
SD-DP			78.13 (2.87)	51.32 (2.95)	89.04 (4.43)	7.22 (0.41)	1.28 (0.04)	4.41 (0.27)	3.42	1.14 (0.02)	14.34 (1.89)

[a]: Leucine concentration calculated as weight% from the total carrier. [b]: NL to carrier weight ratio [c]: $EE_{(f)}$: encapsulation efficiency after recovery of NL from SDP. S_i: initial size, S_f: size following re-dispersion. D[4, 3]: the volume mean diameter and MMAD is the mass median aerodynamic diameter. Results are mean of three determinations (s.d.).

3.2 Mannosylated MXF-NL

Upon linking the biomaromolecule PAM to PE amino group (formula PE2) using the cross-linker gluteraldehyde, the PS and PDI increased significantly to reach 379.32±3.61nm and 0.301±0.045,respectively in PE-PAM, **Table 1**. This probably denoted PAM successful anchoring on the surface liposome surface *via* glutaraldehyde spacer arm. No significant effect on drug EE%, while ζ decreased from -6.54 ± 0.41mV (PE2) to -4.12± 0.32mV (PE-PAM) due to PAM neutral nature contributing probably to the delocalization of the negative charge centers. Similar observations had been previously reported by **[45].** PAM ^{1}H-NMR spectrum, **Fig.1a** reveals a characteristic ϭ values at 6.5 and 6.8, while PE demonstrated no characteristic signals at these ϭ, **Fig. 1b**. The appearance of these signals in PE-PAM spectrum, **Fig.1c**, in spite of their absence in PE characteristic spectrum **Fig. 1b**, confirmed the efficient coupling of PAM to NL.

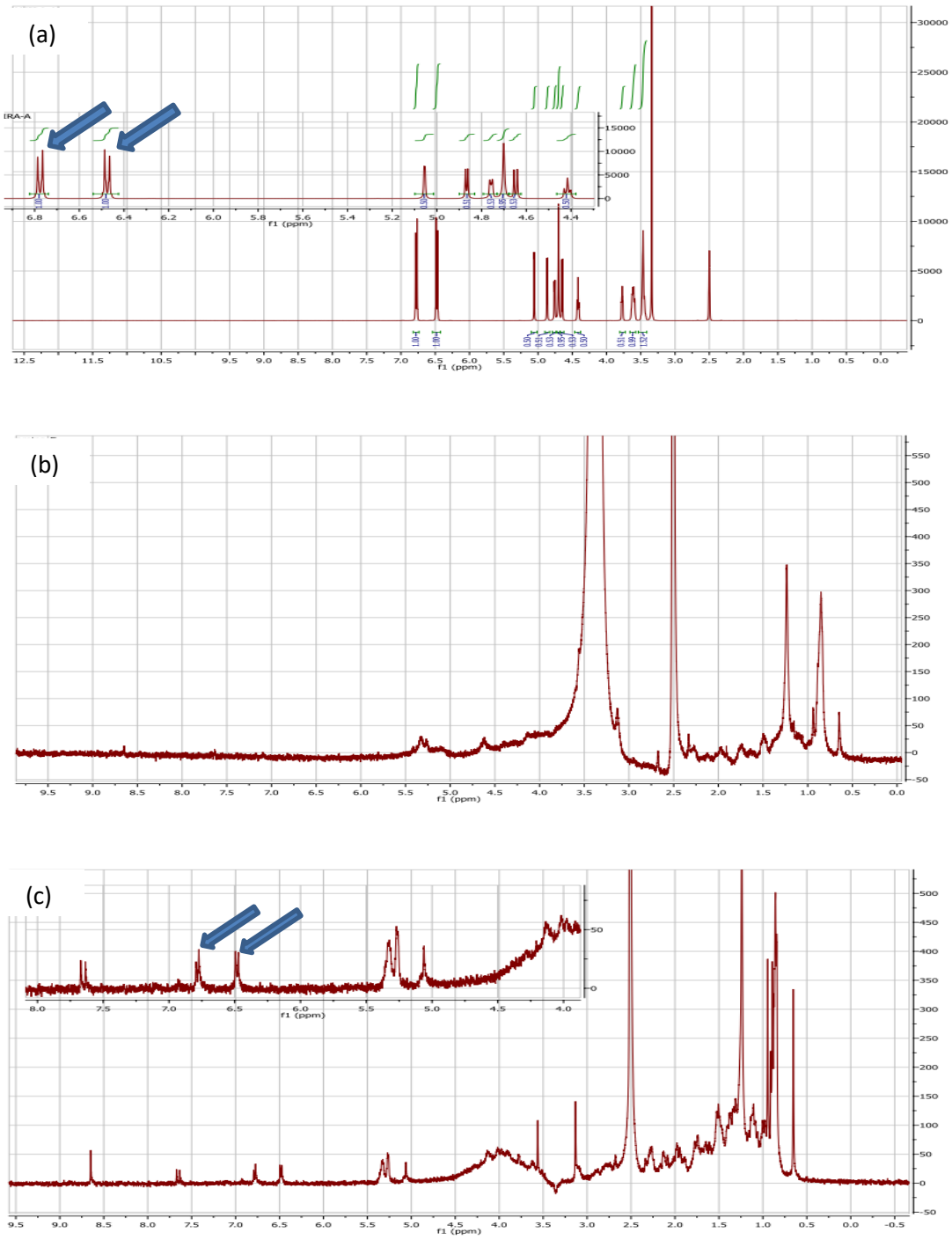

Fig. 1: ^{1}H-NMR spectra of: (a) PAM (b) NL-PE and (c) NL-PE-PAM.

3.3 Morphology of MXF-NL

TEM of NL formulae PC8, DC3 and PE-PAM**, Fig. 2,** show non-agglomerated spherical NL with smooth surfaces. The lipid bilayers in PC and DC appeared as dark ring surrounding the internal brighter aqueous phase **[46]**.

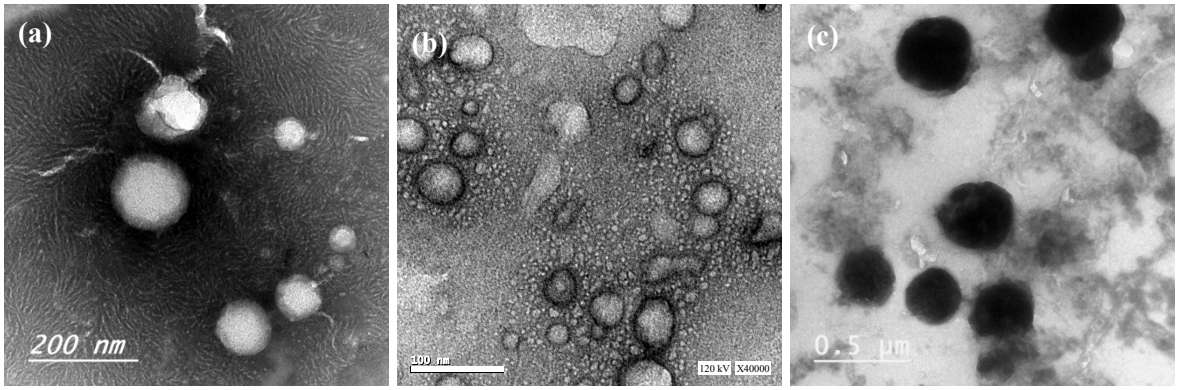

Fig. 2: Transmission elecctron microscope micrographs of selected MXF loaded NL (a) PC8, (b) DC3 and (c) PE-PAM.

3.4 Preparation and characterization of SD-NLEM

3.4.1 Effect of carrier composition

In this study, attempts to *co*-spray dry the selected NL formulae with DX to provide SD-NLEM capable of delivering the drug in the respiratory region. Using DX alone as carrier during spray drying, a low spray drying yield, 46.78 ± 4.39%, was obtained, **Table 2**. Addition of Leu to DX significantly increased the yield% in a concentration dependent manner reaching a maximum% increase of 34% in formula S5 containing 50%w/w Leu. Beyond 50% Leu concentration, only a slight non-significant yield increase *($p>0.05$)* was noted. The anti-adherent properties of Leu probably decreased the cohesive forces between the particles and reduced the adhesion of the powder to the cyclone wall **[47]**. Increasing Leu concentration accompanied by decreasing DX concentration did not significantly affect $\%EE_{(f)}$ of MXF till a 1:1 Leu/DX ratio, beyond which, further increase in Leu/DX ratio significantly reduced the $\%EE_{(f)}$. The presence of a certain concentration of DX is important for keeping liposomal integrity during spray drying **[48]**.

3.4.2. Effect of NL to carrier (NL/C) ratio

Table 2 shows that there was no significant difference between the yields of the various formulae upon varying NL/C ratio (77.88±2.91 to 80.2± 3.93%), while maintaining Leu at 50% concentration. Conversely, the EE was only decreased at a NL/C ratio of 1:2.5 probably due to the insufficiency of the carriers to provide full protection to the NL from the spray drying effects and hence lipid melting and drug leakage of drug from the NL were possible. Similarly, **Fig. 2S** reveals that increasing NL/C ratio from 1:20 (S5) to 1:2.5, (S10) increased S_f/S_i value from 1.03 ± 0.01 to 1.64 ± 0.03, respectively corresponding to more than 60% increase in size .On the other hand, VMD was not affected by NL/C ratio and all SD-NLEM formulae was less than 8μm and the MMAD was less than 5μm pointing to the suitability of the system for alveolar deposition **[49, 50].** A NL/C ratio of 1:7.5 and Leu/DX ratio1:1 was selected for preparing SD-NLEM with various lipids compositions.

3.4.3 Effect of NL composition

Using NL/C ratio of 1:7.5 and Leu/DX ratio1:1 to prepare NL with different lipids compositions yielded SD-NLEM with good and drug AE exceeding 89.04%w/w. The protecting ability of the carrier was confirmed by the non- significantly different $EE_{(f)}$ compared to $EE_{(i)}$, **Table 2.** VMD values ranging from 4.66 ± 0.17 and 7.22 ± 0.41μm with low span values not exceeding 1.28 ± 0.04 were noticed. A desirable MMAD less than 5μm was obtained with all formulae **[51]**. S_f/S_i of all formulae was 1.13 ± 0.02 and 1.14 ± 0.02 with 12.62 ± 2.08 and 14.45 ± 2.07 % increase in size **(Table2).** The PS of the SD-NLEM did not vary significantly following storage six month, see **Fig. 3S**. Irrespective of the lipids used, the residual water contents in the SDP did not exceed 3.42%w/w with non-significant difference among the different formulae, **Table2**.

3.4.5 Particle morphology of SD-NLEM

Irrespective of the type of lipid used, SEM of SD-NLEM formulae, **Fig.3**, show spherical particles with corrugated surfaces and hollow structures inside indicating low density **[52].** This morphology might be acquired from the surface active properties of Leu causing its accumulation on the droplets surface during spray drying. As a hydrophobic SAA, this surface layer will prevent

the passage of water vapor and expand like a balloon. When the water fully evaporates, this layer will collapse producing the observed wrinkled structure with larger inter-particulate separation and low contact areas between the particles **[53, 54]**.

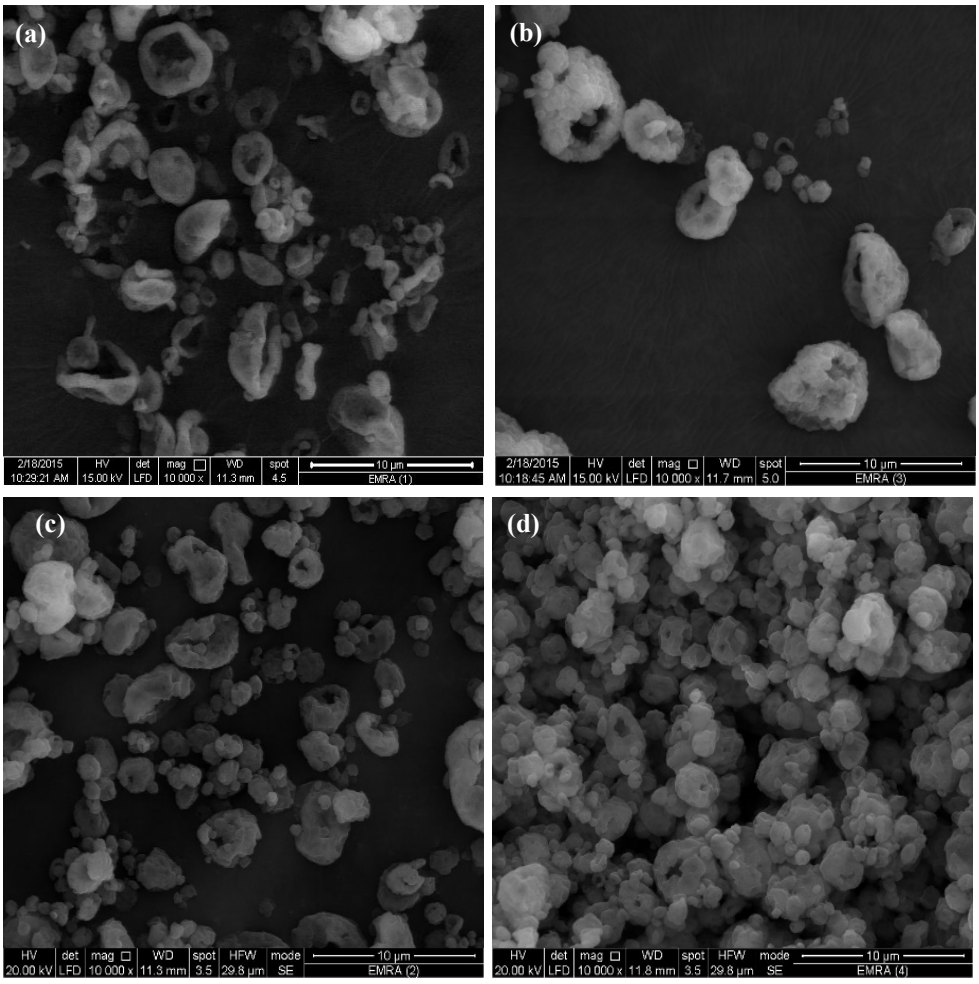

Fig. 3: Scanning electron microscopic images of MXF–SD-NLEM: (a) S8 (SD-PC), (b) SD-PE-PAM, (C) SD-DC and (d) SD-DP.

3.4.6 In vitro aerodynamic deposition using the twin stage glass impinger (TSI)

The EF in all SD-NLEM exceeded 90% denoting the highly dispersible nature of the powders. The FPF, stage 2 deposition, varied from 66.59±4.72 to 72.08±1.07%, **Fig. 4a**. Good aerosolization properties evidenced by the high RP of 69.79±4.31 to 77.97±1.85% for the different SD-NLEM, **Fig.4b**, can be explained based on their SEM. The corrugated surface probably decreased inter-particulate interaction in two ways. First, the asperities prevent close contact between particles. Second, they may reduce the total area accessible for particle' interaction thus decreasing their cohesion and improving their aerosolization properties over the smooth spherical particles of otherwise similar physical properties **[27].**

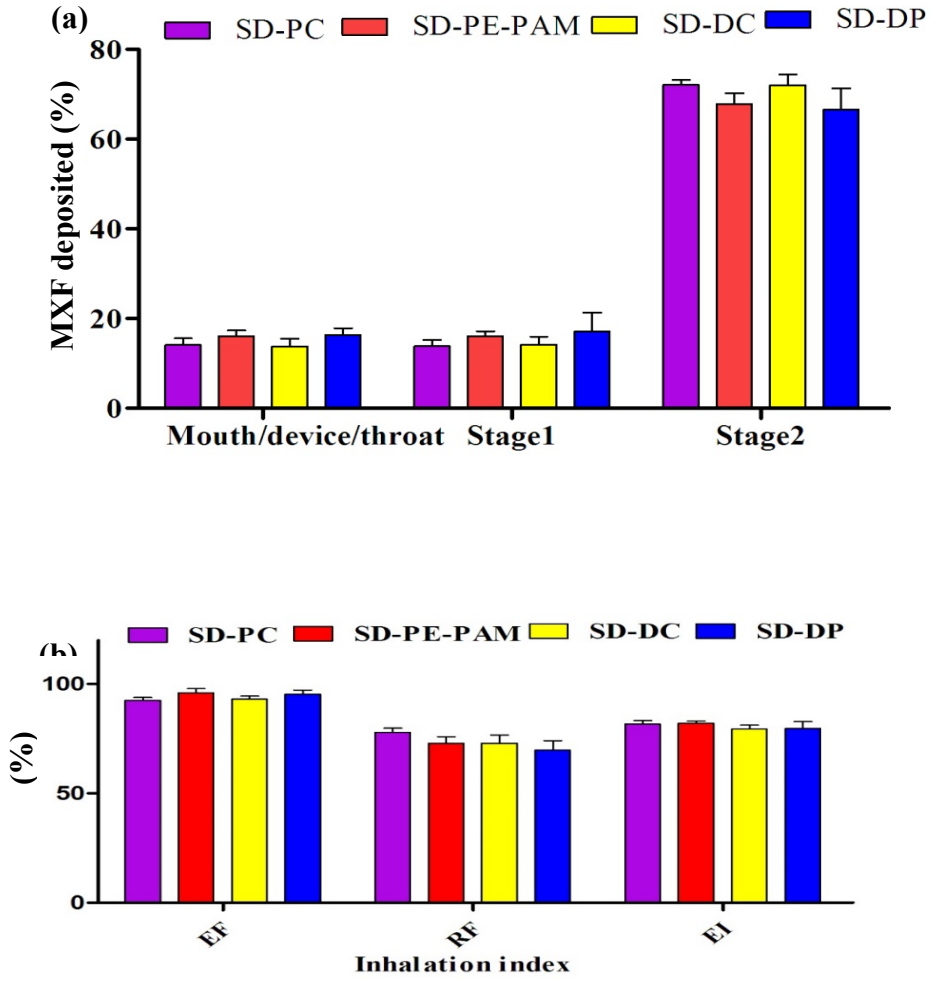

Fig. 4: MXF-SD-NLEM (a) *In vitro* deposition data using TSI and (b) Inhalation indices.

3.4.7 In vitro MXF release from SD-NLEM

As a hydrophilic dug, MXF (98%) was found in the release medium within 3h following dissolution of pure MXF. The release profiles of all tested SD-NLEM were biphasic, showing a relatively fast release intial phase (burst release) over the first two hours amounting from 42.05 to 55.77%, the initial burst release could be attributed to the drug located on the surface and unencapsulated within the NL. This amount was left to start the initial antibacterial drug effect in lung following pulmnary administration. The rate of drug release gradually decreased till~100% of the drug was released within 48h **[55]**. As shown in **Fig. 4S** the release rate was negligibly affected by SD-NLEM type and its lipid composition.

3.4.8 Antibacterial activity of MXF- SD-NLEM

In accordance with literature, MXF solution showed an MIC value of 0.25µg/mL against *M. tuberculosis,* **Table3 [32]**. Conversely, plain SD-NLEM formulae did not exhibit any antibacterial activity against *M. tuberculosis*. **Table 4** shows that SD-DP and SD-DC showed an MIC value of 0.125µg/mL while the neutral SD-NLEM (SD-PC and SD-PE-PAM) exhibited MIC value of 0.25µg/mL similar to that of MXF solution. The two-fold decrease in MIC, in case of charged NL, can be owed to the increased bacterial membrane permeability induced by charged liposome formulation. The cationic NL interacted electrostatically with the negatively charged cell membrane of the mycobacteria and fused with it, enhancing antibacterial activity of the drug **[56]**. The anionic NL, with negatively charged DCP, can form hydrogen bond and/or ionic interaction with various bacterial membrane components *i.e.* saccharide moieties of various natures, phospholipids, glycosphingolipids, lipopolysaccharides and peptidoglycan **[57]**. The interaction and fusion of the liposomes with the bacterial cell membrane enhanced the delivery of the encapsulated drug and eventually improved its antibacterial effectiveness.

3.4.10. Cytotoxicity of SD-NLEM

As shown in **Fig. 5,** the encapsulation of MXF within NL did not induce major difference in cell cytotoxicity when compared with plain formulae. These findings, are considered good indicators of biocompatability and safety of the prepared formulations. **Fig. 5S** evidenced the

safety of lipids used in plain and MXF loaded SD-NLEM at different concentrations on the viability of A549 cells indicating the biocompatibility of the proposed nanocarrier platform.

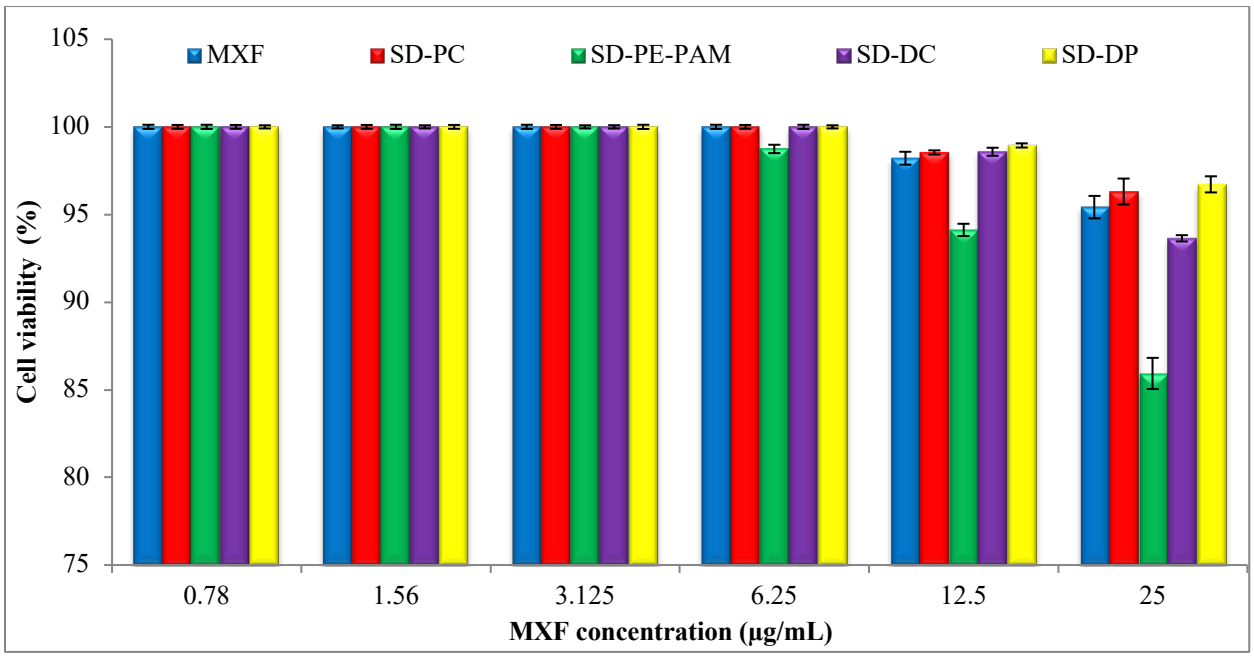

Fig. 5: A549 cell viability measured by MTT cytotoxicity assay after exposure to increasing concentration of MXF-SD-NLEM.

3.4.11. In vitro uptake study using murine mice macrophages J774A.1

FITC loaded liposomes were prepared and spray dried using the same optimized conditions. The amount of FITC entrapped in NL was found to be similar in all formulae (data not shown). **Fig. 6** shows that there was no significant difference between the fluorescent intensity obtained after incubating J774A.1 cells with FITC-labeled NLEM, at two different lipid concentrations (75 and 150 µg/mL), for 3h. At 75 µg/mL of lipid, all SD-NLEM exhibited significantly higher median FI compared to the control and that SD-PE-PAM showed the highest one.

Fig. 7 shows increase in fluorescence level in J774A.1 with time only with the charged liposomal formulations SD-DC and DP. Furthermore, SD-DC and SD-DP exhibited higher mean FI compared to the neutral NL, (SD-PC) denoting the higher macrophage uptake of charged

liposomes**.** Cationic liposomes can interact electrostatically with negatively charged cell membranes and cell surface proteoglycans facilitating their cellular uptake **[58]**. Vyas and *co*-workers reported a 3.4-fold increase in lung retention of rifampicin following its encapsulation in anionic liposomes composed of PC, DCP and CH while only 1.3-fold increase was noted when encapsulated in the corresponding neutral liposomes compared to free drug solution **[59]** .

Although SD-PE-PAM possessed very low negative ζ, nearly neutral, but it showed the highest mean FI with 3.4, 2.32, and 1.6-fold increase in mean FI compared to SD-PC, SD-DP and SD-DC respectively after 3h incubation with J774A.1 cells. Moreover, no time dependence uptake was seen with non-significant difference between the FI at 0.5 and 3h. This fast preferential uptake of SD-PE-PAM might be ascribed to mannosylation as specific receptors of mannose are presented on the surface of AMs **[1].** This result agreed with the findings obtained by **Chono and *co*-workers** who studied the effect of surface mannose modification on aerosolized liposomes delivery to AM **[60].** Other investigators reported similar results upon mannosylation of solid lipid nanoparticles **[61]** and polypropyleneimine dendrimers **[62]**.

3.4.12. In vivo pulmonary deposition of SD-NLEM

One representative formula (SD-PC) was selected for studying the *in vivo* deposition pattern following intrapulmonary administration of fluorescent SD-NLEM using DPI from *Penn-century*®. **Fig. 8a** shows the green fluorescence of FITC- SD-NLEM. The auto-fluorescence of the rat lung was found to be low except in the peripheral regions where pulmonary artery gave a bright auto-fluorescence as shown in **Fig. 8b [63].** Few fluorescently green particles appeared in the trachea and bronchus, **Fig. 8c and d**, while several green spots were evident in the alveolar ducts and spaces**, Fig. 8e and f.** This indicated that the developed SD-NLEM were localized mainly in the alveolar spaces and nearly absent or showed very low deposition in the upper respiratory tract (trachea and bronchi). From a therapeutic point of view, the deposition of high percentage SD-NLEM in alveolar space is so important as it is the site where *mycobacterium tuberculosis* (*M. tuberculosis*) can reside and survive for extended period of time **[5]**.

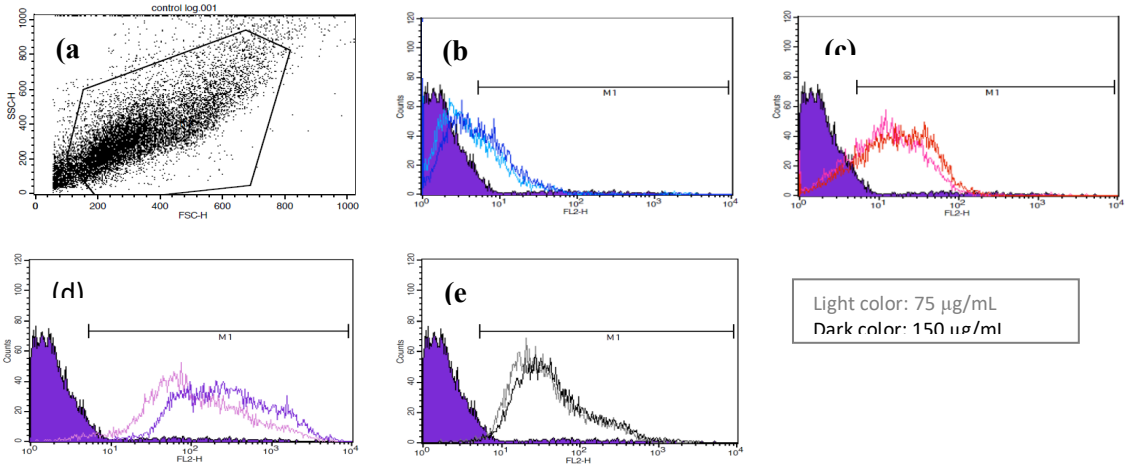

Fig. 6: Flow cytometry diagram of (a) control murine macrophages (J774A.1) and murine macrophages (J774A.1) after exposure for 3h to (b) SD-PC, (c) SD-PE-PAM, (d) SD-DC and (e) SD-DP at different lipid concentrations.

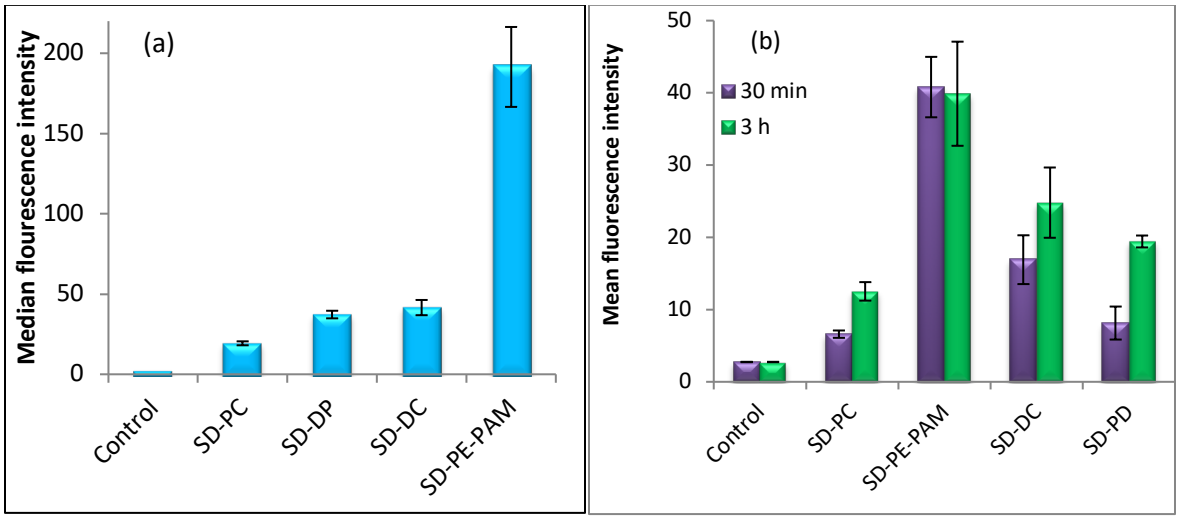

Fig. 7: (a) Median fluorescence intensity obtained after incubation of J774A.1 cells with selected fluorescently labeled MXF-NL formulae for 3h using a lipid concentration of 75 µg/mL and (b) Mean fluorescence intensity obtained after incubation of J774A.1 cells with different MXF-SD-NLEM formulae for different time intervals.

4. Conclusion

At a PC/CH ratio of 7:3, NL exhibited the highest EE% and lowest PDI with a small PS. The antibacterial activity of MXF against *M. tuberculosis* was maintained by encapsulation in liposomes and was enhanced upon using charged liposomes. The chosen spray drying parameters and the selected excipients guaranteed low moisture content in SD-NLEM and enhanced the physical stability of liposomes. *In vitro* data, substantiated by *in vivo* studies, confirmed that the PS and morphological characteristics of the spray dried powders allowed for high deposition of the particles in the alveolar region where the microorganism resides. The presence of DCP and DOTAP potentiated the drug anti- mycobacterial activity. PAM surface decoration enhanced the active uptake by alveolar macrophages. Using this passively targeted carrier system, to actively target to the most difficult infection where the micro-organism is hidden in the macrophages. The enhanced stability, therapeutic efficiency, and improved deep lung deposition, evidenced by *in vivo* data, elected the system for use in severe cases of intracellular diseases.

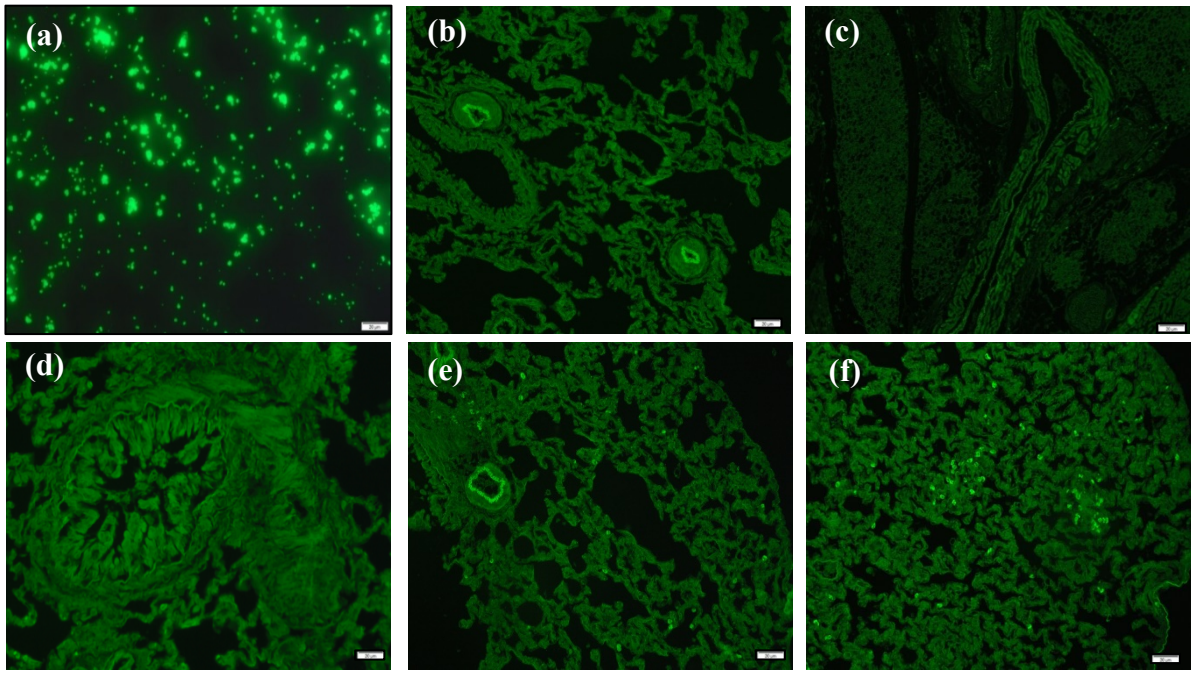

Fig. 8: Fluorescent microscopic images of (a) FITC labeled SD-NLEM (Formula S8) and (b) rat lung tissue (control) (The bright region corresponds to the pulmonary artery) and *in vivo* deposition of FITC labeled SD-NLEM (SD-PC) in rat lung sections (c) trachea, (d) bronchia, (e) and (f) alveolar ducts. The images are representative of 3-5 slides per each area, scale bar represents 20 µm.

Acknowledgments

The authors would also like to thank Dr Rebecca Klippstein, King's College London for technical assistance with J774 uptake study. Special thanks to the Post Graduate sector-Ain Shams University for the Partial Fund granted to the present work.

References

[1] G.K. Saraogi, B. Sharma, B. Joshi, P. Gupta, U.D. Gupta, N.K. Jain, G.P. Agrawal, Journal of drug targeting, 19 (2011) 219-227.
[2] Q. Zhou, S.S.Y. Leung, P. Tang, T. Parumasivam, Z.H. Loh, H.-K. Chan, Advanced Drug Delivery Reviews, 85 (2015) 83-99.
[3] D.-D. Pham, E. Fattal, N. Tsapis, International Journal of Pharmaceutics, 478 (2015) 517-529.
[4] S.M. Hwang, D.D. Kim, S.J. Chung, C.K. Shim, Journal of Controlled Release, 129 (2008) 100-106.
[5] J.-H. Park, H.-E. Jin, D.-D. Kim, S.-J. Chung, W.-S. Shim, C.-K. Shim, International Journal of Pharmaceutics, 441 (2013) 562-569.
[6] E. Elmowafy, R. Osman, R.A. Ishak, Current pharmaceutical design, 23 (2017) 373-392.
[7] Y. Tang, H. Zhang, X. Lu, L. Jiang, X. Xi, J. Liu, J. Zhu, Drug delivery, 22 (2015) 608-618.
[8] C. Kelly, C. Jefferies, S.A. Cryan, J Drug Deliv, 727241 (2011) 26.
[9] J. Cheng, J.A. Thanassi, C.L. Thoma, B.J. Bradbury, M. Deshpande, M.J. Pucci, Antimicrobial agents and chemotherapy, 51 (2007) 2445.
[10] M.T. Heinrichs, G.L. Drusano, D.L. Brown, M.S. Maynard, S.K.B. Sy, K.H. Rand, C.A. Peloquin, A. Louie, H. Derendorf, International journal of antimicrobial agents, (2018).
[11] C. de Miranda Silva, A. Hajihosseini, J. Myrick, J. Nole, A. Louie, S. Schmidt, G.L. Drusano, Antimicrobial agents and chemotherapy, 63 (2019).
[12] L. Sercombe, T. Veerati, F. Moheimani, S.Y. Wu, A.K. Sood, S. Hua, Frontiers in pharmacology, 6 (2015) 286-286.
[13] M.V. Vadakkan, K. Annapoorna, K.C. Sivakumar, S. Mundayoor, G.S. Kumar, Int J Nanomedicine, 8 (2013) 2871-2885.
[14] M. Gandhi, T. Pandya, R. Gandhi, S. Patel, R. Mashru, A. Misra, H. Tandel, International Journal of Pharmaceutics, 496 (2015) 886-895.
[15] T. Handa, H. Takeuchi, Y. Ohokubo, Y. Kawashima, CHEMICAL & PHARMACEUTICAL BULLETIN, 35 (1987) 748-755.
[16] Kulkarni, G.V. Betageri, M. Singht, J. MICROENCAPSULATION, 12, NO. 3, (1995) 229-246
[17] S.P. Vyas, S. Quraishi, S. Gupta, K.S. Jaganathan, International Journal of Pharmaceutics, 296 (2005) 12-25.
[18] A. Wieber, T. Selzer, J. Kreuter, International Journal of Pharmaceutics, 421 (2011) 151-159.
[19] P. Ghosh, P.K. Das, B.K. Bachhawat, Archives of Biochemistry and Biophysics, 213 (1982) 266-270.
[20] S.P. Vyas, Y.K. Katare, V. Mishra, V. Sihorkar, International Journal of Pharmaceutics, 210 (2000) 1-14.
[21] V.P. Torchilin, B.A. Khaw, V.N. Smirnov, E. Haber, Biochemical and biophysical research communications, 89 (1979) 1114-1119.
[22] F. Maestrelli, M.L. González-Rodríguez, A.M. Rabasco, P. Mura, International Journal of Pharmaceutics, 298 (2005) 55-67.
[23] R. Osman, P.L. Kan, G. Awad, N. Mortada, A.E. El-Shamy, O. Alpar, International journal of pharmaceutics, 449 (2013) 44-58.
[24] M. Chougule, B. Padhi, A. Misra, AAPS PharmSciTech, 9 (2008) 47-53.

[25] A.J. Kundawala, V.A. Patel, H.V. Patel, D. Choudhary, International Journal of Pharmaceutical Sciences & Drug Research, 3 (2011) 297.
[26] Kho, Katherine, Hadinoto, Kunn, Colloids and Surfaces A: Physicochemical and Engineering Aspects, 359 (2010) 71-81.
[27] H. Yu, J. Teo, J.W. Chew, K. Hadinoto, International Journal of Pharmaceutics, 499 (2016) 38-46.
[28] A.F. Ourique, S. Chaves Pdos, G.D. Souto, A.R. Pohlmann, S.S. Guterres, R.C. Beck, European journal of pharmaceutical sciences : official journal of the European Federation for Pharmaceutical Sciences, 65 (2014) 174-182.
[29] R. Osman, P.L. Kan, G. Awad, N. Mortada, A.-E. El-Shamy, O. Alpar, International Journal of Pharmaceutics, 449 (2013) 44-58.
[30] M.D. Louey, S. Razia, P.J. Stewart, International Journal of Pharmaceutics, 252 (2003) 87-98.
[31] M. Singh, D.S. Chauhan, P. Gupta, R. Das, R.K. Srivastava, P. Upadhyay, P. Singh, K. Srivastava, J. Faujdar, G.P. Jaudaun, V.S. Yadav, V.D. Sharma, K. Venkatesan, S. Sachan, P. Sachan, K. Katoch, V.M. Katoch, The Indian journal of medical research, 129 (2009) 542-547.
[32] S.H. Gillespie, O. Billington, The Journal of antimicrobial chemotherapy, 44 (1999) 393-395.
[33] D.P. Gaspar, V. Faria, L.M. Goncalves, P. Taboada, C. Remunan-Lopez, A.J. Almeida, International journal of pharmaceutics, 497 (2016) 199-209.
[34] M.L. Manca, D. Valenti, O.D. Sales, A. Nacher, A.M. Fadda, M. Manconi, International Journal of Pharmaceutics, 472 (2014) 102-109.
[35] D. Singodia, A. Verma, R.K. Verma, P.R. Mishra, Nanomedicine: Nanotechnology, Biology and Medicine, 8 (2012) 468-477.
[36] W. Wijagkanalan, S. Kawakami, M. Takenaga, R. Igarashi, F. Yamashita, M. Hashida, Journal of Controlled Release, 125 (2008) 121-130.
[37] F. Ungaro, C. Giovino, C. Coletta, R. Sorrentino, A. Miro, F. Quaglia, European Journal of Pharmaceutical Sciences, 41 (2010) 60-70.
[38] F. Ungaro, I. d'Angelo, C. Coletta, R. d'Emmanuele di Villa Bianca, R. Sorrentino, B. Perfetto, M.A. Tufano, A. Miro, M.I. La Rotonda, F. Quaglia, Journal of Controlled Release, 157 (2012) 149-159.
[39] Z.S. Haidar, R.C. Hamdy, M. Tabrizian, Biomaterials, 29 (2008) 1207-1215.
[40] K. Moribe, K. Maruyama, M. Iwatsuru, International Journal of Pharmaceutics, 193 (1999) 97-106.
[41] C. Socaciu, R. Jessel, H.A. Diehl, Chemistry and Physics of Lipids, 106 (2000) 79-88.
[42] V.B. Patel, A.N. Misra, j. microencapsulation, 16 (1999) 357-367.
[43] M.-X. Chen, B.-K. Li, D.-K. Yin, J. Liang, S.-S. Li, D.-Y. Peng, Carbohydrate Polymers, 111 (2014) 298-304.
[44] S. Lemaire, P.M. Tulkens, F. Van Bambeke, Antimicrobial agents and chemotherapy, 55 (2011) 649-658.
[45] X. Ying, H. Wen, W.-L. Lu, J. Du, J. Guo, W. Tian, Y. Men, Y. Zhang, R.-J. Li, T.-Y. Yang, D.-W. Shang, J.-N. Lou, L.-R. Zhang, Q. Zhang, Journal of Controlled Release, 141 (2010) 183-192.
[46] M. Elmowafy, T. Viitala, H.M. Ibrahim, S.K. Abu-Elyazid, A. Samy, A. Kassem, M. Yliperttula, European Journal of Pharmaceutical Sciences, 50 (2013) 161-171.

[47] P.H. Moghaddam, V. Ramezani, E. Esfandi, A. Vatanara, M. Nabi-Meibodi, M. Darabi, K. Gilani, A.R. Najafabadi, Powder Technology, 239 (2013) 478-483.
[48] R.A. Ishak, R. Osman, G.A. Awad, Current pharmaceutical design, 22 (2016) 3411-3428.
[49] R.J. Malcolmson, J.K. Embleton, Pharmaceutical Science & Technology Today, 1 (1998) 394-398.
[50] M.Y. Yang, J.G.Y. Chan, H.-K. Chan, Journal of Controlled Release, 193 (2014) 228-240.
[51] B.Y. Shekunov, P. Chattopadhyay, H.H. Tong, A.H. Chow, Pharmaceutical research, 24 (2007) 203-227.
[52] B. Cuvelier, P. Eloy, C. Loira-Pastoriza, B. Ucakar, A.A. Sanogo, C. Dupont-Gillain, R. Vanbever, International Journal of Pharmaceutics, 495 (2015) 981-990.
[53] M. Mishra, B. Mishra, Yakugaku zasshi : Journal of the Pharmaceutical Society of Japan, 131 (2011) 1813-1825.
[54] K. Kaewjan, T. Srichana, Pharmaceutical development and technology, 21 (2016) 68-75.
[55] M.M. Nounou, E.-k. Labib K, K. Nawal , K. Said A, Acta Pharm., 56 (2006) 311-324.
[56] Z. Drulis-Kawa, J. Gubernator, A. Dorotkiewicz-Jach, W. Doroszkiewicz, A. Kozubek, Cellular & molecular biology letters, 11 (2006) 360-375.
[57] P.M. Furneri, M. Fresta, G. Puglisi, G. Tempera, Antimicrobial agents and chemotherapy, 44 (2000) 2458-2464.
[58] A. Wieber, T. Selzer, J. Kreuter, European Journal of Pharmaceutics and Biopharmaceutics, 80 (2012) 358-367.
[59] S.P. Vyas, M.E. Kannan, S. Jain, V. Mishra, P. Singh, International Journal of Pharmaceutics, 269 (2004) 37-49.
[60] S. Chono, K. Kaneko, E. Yamamoto, K. Togami, K. Morimoto, Drug development and industrial pharmacy, 36 (2010) 102-107.
[61] N. Nimje, A. Agarwal, G.K. Saraogi, N. Lariya, G. Rai, H. Agrawal, G.P. Agrawal, Journal of drug targeting, 17 (2009) 777-787.
[62] P.V. Kumar, A. Asthana, T. Dutta, N.K. Jain, Journal of drug targeting, 14 (2006) 546-556.
[63] C. Bosquillon, V. Préat, R. Vanbever, Journal of Controlled Release, 96 (2004) 233-244.